

See discussions, stats, and author profiles for this publication at: <https://www.researchgate.net/publication/221720539>

# Synthesis and Self-Assembly of Au@SiO<sub>2</sub> Core-Shell Colloids

ARTICLE · JULY 2002

---

CITATIONS

37

---

READS

53

4 AUTHORS, INCLUDING:



Lu Yu

University of California, Riverside

37 PUBLICATIONS 4,037 CITATIONS

SEE PROFILE



Yadong Yin

University of California, Riverside

269 PUBLICATIONS 23,260 CITATIONS

SEE PROFILE

# Synthesis and Self-Assembly of Au@SiO<sub>2</sub> Core–Shell Colloids

Yu Lu,<sup>†</sup> Yadong Yin,<sup>†</sup> Zhi-Yuan Li,<sup>‡</sup> and Younan Xia<sup>\*,‡</sup>

*Department of Materials Science and Engineering, and Department of Chemistry,  
University of Washington, Seattle, Washington 98195*

*Received April 30, 2002*

## ABSTRACT

Gold nanoparticles have been coated with amorphous silica to form spherical colloids with a core–shell structure. The thickness of silica shells could be conveniently controlled in the range of tens to several hundred nanometers by changing the concentration of the sol–gel precursor or the coating time. These core–shell colloids could serve as the building blocks to fabricate photonic devices. In one demonstration, we showed that these core–shell particles could be assembled into long-range ordered lattices (or photonic crystals) over large areas that exhibited optical properties different from those crystallized from silica colloids. Transmission spectra of these crystals displayed both features that correspond to the Bragg diffraction of a periodic lattice and the plasmon resonance absorption of gold nanoparticles. Reflectance spectra taken from these crystals only showed peaks caused by Bragg diffraction. In another demonstration, these core–shell colloids were assembled into chains of different configurations by templating against well-defined channels patterned in thin films of photoresist. As suggested by previous studies, the plasmon coupling between gold cores makes these structures ideal candidates for nanoscale waveguides with lateral mode sizes well below the optical diffraction limit.

Metal nanoparticles have been the subject of extensive research due to their unique applications in many areas such as nonlinear optical switching,<sup>1</sup> immunoassay labeling,<sup>2</sup> and Raman spectroscopy enhancement.<sup>3</sup> Gold and silver colloids are probably the most studied and best established systems, and a variety of procedures have been developed to process them as stable dispersions characterized by relatively small size variations.<sup>4</sup> The properties of these colloids can be further tailored by coating their surfaces with uniform, conformal shells made of dielectric materials such as silica.<sup>5</sup> In principle, one can achieve a precise control over the optical properties of these core–shell colloids by fine-tuning the chemical composition, structure, and dimensions of the cores or shells.<sup>6</sup> For coating gold or silver nanoparticles with amorphous silica shells, Mulvaney et al. have reported a three-step procedure that involved the use of an amine-terminated silane coupling agent as the primer to render the gold surfaces vitreophilic.<sup>7</sup> Matijevic et al. later found that it was also possible to form uniform coatings of silica on silver nanoparticles without derivatizing their surfaces with any coupling agent.<sup>8</sup> More recently, we demonstrated that a slightly modified Stöber (or sol–gel) process could be directly applied to coat iron oxide nanoparticles or silver nanowires with well-controlled silica shells or sheaths.<sup>9</sup> Here we further illustrate that this procedure can be extended to coat gold nanoparticles with silica shells of well-controlled

thickness without using a primer. In addition to the demonstration of this coating process, we have also explored the potential use of these core–shell colloids as building blocks in self-assembly to fabricate functional optical devices such as photonic crystals and plasmonic waveguides.

Our initial effort was focused on the coating of gold nanoparticles (with an average diameter of 50 nm) obtained from Ted Pella (Redding, CA). As shown by their TEM image in Figure 1A, these gold nanoparticles were characterized by a range of different morphologies, although they were relatively uniform in size (with a coefficient of variation ~10%). We could directly coat the surfaces of these gold nanoparticles with conformal shells of amorphous silica using the sol–gel process reported previously.<sup>9</sup> In this process, the formation of silica coatings involved base-catalyzed hydrolysis of tetraethyl orthosilicate (TEOS) to generate silica sols, followed by nucleation and condensation of these sols onto the surfaces of gold nanoparticles. Ammonia could be added as a catalyst to speed up the hydrolysis of TEOS precursor. In a typical procedure, 4 mL gold colloids (50 nm in diameter,  $4.5 \times 10^{10}$  particles/mL) was added to 20 mL 2-propanol. Under continuous stirring, 0.5 mL ammonia solution (30wt %, Aldrich) and various amounts of TEOS (0.004–0.01 M, Aldrich, used as-received) were consecutively added to the reaction mixture. The reaction was allowed to proceed for ~1 h at room temperature under continuous stirring. Due to the presence of negative charges on the surfaces of silica shells, the product could be well-

\* Corresponding author. E-mail: xia@chem.washington.edu.

<sup>†</sup> Department of Materials Science and Engineering.

<sup>‡</sup> Department of Chemistry.

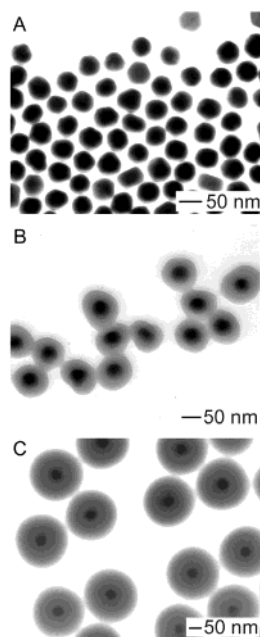


**Figure 1.** (A) Transmission electron microscopy (TEM) image of gold nanoparticles with an average diameter of 50 nm. (B, C) TEM images of such gold nanoparticles after their surfaces had been coated with amorphous silica shells of  $\sim 20$  and  $\sim 80$  nm in thickness, respectively.

dispersed in water without adding any surfactant. The core-shell particles could be separated from the reaction medium by centrifuging at  $\sim 4000$  rpm and then redispersed into deionized water. By controlling experimental conditions, for example, the coating time and the concentration of catalyst, water, or precursor, we were able to vary the shell thickness in the range of tens to several hundred nanometers.<sup>9</sup> Figure 1B shows the TEM image of gold nanoparticles after they had been coated with amorphous silica shells of  $\sim 20$  nm in thickness. At this stage, the core-shell colloids still exhibited the original morphologies of gold cores, together with a relatively large variation in size. When the silica coatings had a thickness comparable to the diameter of gold cores, the core-shell particles became essentially monodispersed in size (with a coefficient of variation less than 2%, as determined from TEM and SEM images containing more than 500 particles); they also exhibited a spherical shape regardless of the morphologies of original gold cores. As shown in Figure 1C, each silica shell had a uniform cross-section over the entire surface of gold core when the shell thickness was increased to  $\sim 80$  nm.

Because of their spherical shapes and small variation in size, these core-shell colloids could serve as building blocks to fabricate three-dimensional photonic crystals. Due to the existence of plasmon resonance absorption of gold cores, the optical properties of these crystals are expected to be different from those of crystals assembled from silica or polymer beads.<sup>10</sup> Figure 2A shows the SEM image of a crystalline lattice made of Au@SiO<sub>2</sub> colloids. The gold cores were 50 nm in diameter and silica shells had a thickness of 100 nm (as measured from TEM images). This three-dimensionally ordered lattice had a face-center-cubic (fcc) structure, with its (111) planes oriented parallel to the

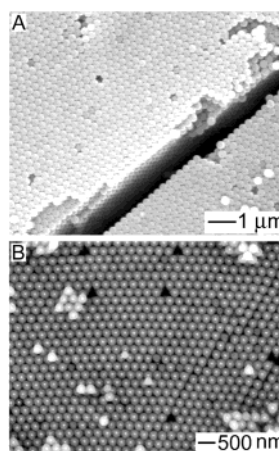


**Figure 2.** (A) The scanning electron microscope (SEM) image of a photonic crystal crystallized from Au/SiO<sub>2</sub> nanoparticles that had cores of 50 nm in diameter and shells  $\sim 80$  nm in thickness. (B) Backscattering SEM image of this crystal, showing that there was a gold core within each core-shell colloidal particle.

supporting substrate. The crack shown in this SEM image was formed due to volume shrinkage when the sample was dried. We have tested a number of ways to organize these Au@SiO<sub>2</sub> core-shell colloids into crystalline lattices and found that they could be readily assembled into opaline lattices in a microfluidic cell constructed by sandwiching a rectangular gasket ( $\sim 20$   $\mu\text{m}$  thick, cut out of the Mylar film) between two glass substrates.<sup>11</sup> In a typical procedure, a hole of  $\sim 3$  mm in diameter was generated in the top substrate by drilling with a diamond-coated tool, and a glass tube ( $\sim 6$  mm in diameter) was attached to this hole using epoxy adhesive. Both glass substrates were treated with oxygen plasma for a few minutes to make their surfaces hydrophilic. The cell was assembled in a clean room and held together with several binder clips. After the glass tube had been filled with an aqueous dispersion of Au@SiO<sub>2</sub> colloids, its opening was covered with Para film to prevent solvent from evaporation. The Au@SiO<sub>2</sub> spherical colloids were forced to enter the packing cell via capillary action, concentrated at all edges of the gasket through solvent removal, and crystallized into a long-range ordered lattice under continuous sonication. Depending on the thickness of the gasket, we could obtain opaline crystals of  $\sim 20$ - $\mu\text{m}$  thick over  $\sim 1$  cm<sup>2</sup> within a few days. Figure 2B shows the backscattering SEM image of the (111) plane of this crystalline lattice, clearly indicating the existence of a gold core in the middle of each colloidal particle.

We have characterized the optical properties of these aqueous dispersions of Au@SiO<sub>2</sub> core-shell colloids and their crystalline lattices using UV-visible spectroscopy. Figure 3A shows the absorption spectra of aqueous dispersions of Au@SiO<sub>2</sub> colloids with different shell thicknesses. Before coating, the gold nanoparticles had a characteristic surface plasmon peak at  $\sim 528$  nm. Because the refractive index of silica is slightly higher than that of water, this plasmon peak was red shifted to  $\sim 540$  nm when the surfaces of these gold nanoparticles were coated with silica shells. The position of this peak was not sensitive to the change in coating thickness, while its intensity increased accordingly

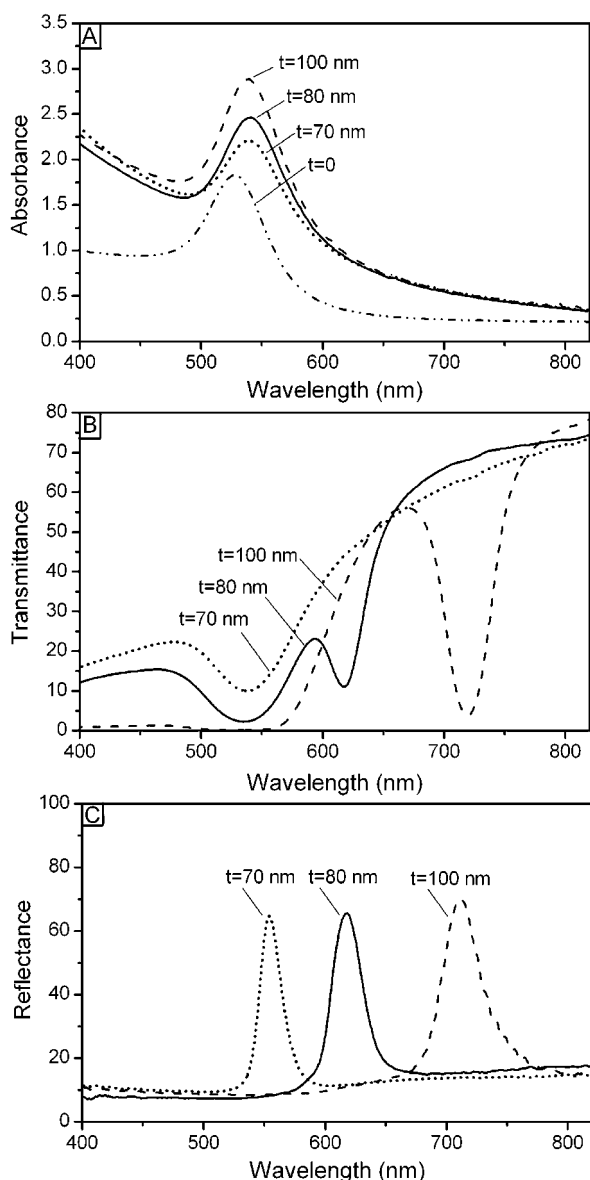


**Figure 3.** (A) UV–visible absorption spectra of aqueous dispersions that contained Au@SiO<sub>2</sub> core–shell nanoparticles with different shell thickness ( $t$ ). The gold cores were 50 nm in diameter for all samples. (B, C) Transmission and reflectance spectra taken from photonic crystals crystallized from these Au@SiO<sub>2</sub> core–shell particles. The incident light was perpendicular to the (111) planes of these face-center-cubic crystalline lattices for all measurements.

as thicker silica shells were formed. This last observation differed from the results of a previous study by Mulvaney et al.,<sup>12</sup> in which the plasmon peak was completely masked by the scattering of the core–shell colloids once the shell thickness had reached a value of  $\sim 80$  nm. Figure 3B shows the transmission spectra of opaline lattices assembled from these Au@SiO<sub>2</sub> particles. When taking these spectra, all samples were wet with the void spaces among particles being completely filled with water. The incident light was kept perpendicular to the (111) planes of these face-center-cubic lattices. These transmission spectra show both peaks originated from the plasmon resonance of gold cores (at  $\sim 540$  nm) and the Bragg diffraction of each opaline lattice. The

position of the Bragg diffraction peak varied as the thickness of silica shell changed. When the silica shell was 70 nm in thickness, the Bragg diffraction peak overlapped with the plasmon resonance band. In this case, only one broad absorption peak was observed at 540 nm. Figure 3C shows the reflection spectra taken from the same crystals, with both incident and reflected light oriented perpendicular to the (111) planes. In this configuration, only the Bragg diffraction features were detected, and their positions matched very well with those recorded in the transmission spectra. As expected, the Bragg diffraction peak (associated with the sample having shell thickness of 70 nm) that overlapped with the plasmon resonance band in the transmission mode showed up in the reflectance spectrum as a well-resolved narrow peak. We note that Liz-Marzan et al. have recently demonstrated the fabrication of 3D crystalline lattices from Au@SiO<sub>2</sub> core–shell colloids, albeit no optical measurement was reported in their publication.<sup>10c</sup>

Another interesting application for the Au@SiO<sub>2</sub> core–shell colloids is their use as building blocks to fabricate plasmonic waveguides with nanoscale lateral dimensions. Computational studies by several groups have illustrated that electromagnetic (EM) energy can be transported through linear chains of metal (such as gold and silver) nanoparticles with a spatial confinement well below optical diffraction limit (in the subwavelength region).<sup>13</sup> The major requirement is that these particles are separated by gaps narrow enough to allow for near-field coupling between the plasmon resonance modes associated with adjacent metal nanoparticles.<sup>14</sup> Numerical simulations further indicated that coherent propagation of EM energy with group velocities exceeding  $0.1c$  was also possible in plasmon waveguides containing sharp corners as long as the curvature of bending is smaller than the wavelength of visible light.<sup>15</sup> In a recent publication, Atwater et al. described two methods for fabricating such plasmonic waveguides by employing either electron beam lithography or atomic force microscopic manipulation.<sup>16</sup> Although e-beam writing can routinely generate linear arrays of gold nanoparticles with well-controlled dimensions and spatial separations, the development of this technique into a practical method for producing large numbers of such nanostructures rapidly and at low-cost still requires great ingenuity. When compared with e-beam lithography, the manipulation method based on scanning force microscopy seems to be even more limited in terms of accuracy, efficiency, flexibility, speed, and yield. As a result, it is still highly desired to develop alternative routes to the fabrication of this new type of waveguiding nanostructure.

In a recent work, we have established that physical confinement and attractive capillary forces can be combined to provide an effective strategy for organizing monodispersed spherical colloids into one-dimensional aggregates with well-defined structures.<sup>17</sup> When Au@SiO<sub>2</sub> core–shell colloids were used as the building blocks, plasmonic waveguiding structures with different geometric configurations could be fabricated rapidly in prototype forms. Figure 4 shows SEM images of two typical examples of plasmonic waveguides that are characterized by circular and rectangular curvatures,



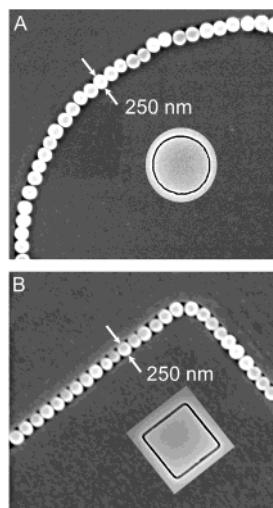


**Figure 4.** SEM images of plasmonic waveguide structures fabricated by assembling the Au@SiO<sub>2</sub> core-shell particles against templates (see insets) patterned in thin films of photoresist. These core-shell particles had a core diameter of 50 nm and a shell thickness of  $\sim 100$  nm.

respectively. In a typical fabrication procedure, aqueous dispersions of the Au@SiO<sub>2</sub> core-shell particles were allowed to dewet across photoresist films whose surfaces had been patterned with 2D arrays of appropriate templates (as shown in insets) using near-field optical lithography.<sup>18</sup> These core-shell colloids were trapped by the templates and assembled into chains with closed packed structures. The configuration of the assembled chains was determined by the geometric confinement provided by the templates. As suggested in the literature, the practical fabrication method for such plasmon waveguides should be able to produce metal nanoparticles with a narrow size distribution and a regular and well-controlled spacing between particles.<sup>16</sup> Our approach could easily meet these requirements. First, recent developments in particle synthesis and physical characterization have enabled the production of metal nanoparticles with very uniform shapes and well-controlled dimensions.<sup>4</sup> Detailed synthesis procedures (as well as commercial products) are readily accessible. Second, the sol-gel procedure described in this paper has allowed us to coat these core particles with uniform silica shells of controllable thickness. When assembled under the confinement of channel-like templates, the core nanoparticles should be evenly spaced by the silica shells (as shown in Figure 4), and the spacing between adjacent gold cores could be conveniently controlled by changing the thickness of silica shells. Another interesting advantage of the present approach is that multiple waveguiding structures with various geometries can be fabricated in a single step by designing templates containing appropriate test patterns.

In summary, we have demonstrated that gold nanoparticles could be directly coated with uniform shells of amorphous silica using a sol-gel process. The thickness of such a conformal coating could be changed from tens to several hundred nanometers by controlling the concentration of TEOS precursor or the deposition time. The potential use of these spherical, core-shell colloids in fabricating photonic

devices has been illustrated with two examples: photonic crystals and plasmonic waveguides. Both optical performance and efficiency of these photonic devices could be controlled by changing the thickness of silica shells and the diameter of gold cores. These demonstrations suggest that Au@SiO<sub>2</sub> core-shell particles with well-controlled sizes are promising building blocks for nanoscale integrated optics, in which the dimensions of structures for guiding and modulating photons will no longer be limited by the wavelength of light.

**Acknowledgment.** This work has been supported in part by the Office of Naval Research (N-00014-01-1-0976), a Career Award from the National Science Foundation (DMR-9983893), and a Fellowship from the David and Lucile Packard Foundation. Y.X. is a Research Fellow of the Alfred P. Sloan Foundation (2000-2002). Y.Y. thanks the Center for Nanotechnology at the UW for a Graduate Research Fellowship.

## References

- (1) Carotenuto, G.; Pepe, G. P.; Nicolais, L. *Eur. Phys. J. B* **2000**, *16*, 11.
- (2) Gavazzi, I.; Nermut, M. V.; Marchisio, P. C. *J. Cell Sci.* **1989**, *94*, 85.
- (3) (a) Wei, A.; Kim, B.; Sadler, B.; Tripp, S. L. *Chem. Phys. Chem.* **2001**, *2*, 743. (b) Fornasiero, D.; Grieser, F. J. *Colloid Interface Sci.* **1991**, *141*, 168. (c) Haynes, C. L.; Van Duyne, R. P. *J. Phys. Chem. B* **2001**, *105*, 5599.
- (4) Handley, D. A. In *Colloidal Gold: Principles, Methods, and Applications*; Hayat, M. A., Ed.; Academic Press: San Diego, 1989.
- (5) (a) Mayya, K. S.; Gittins, D. I.; Caruso, F. *Chem. Mater.* **2001**, *13*, 3833. (b) Liz-Marzan, L. M.; Mulvaney, P. *New J. Chem.* **1998**, *22*, 1285. (c) Wang G.; Harrison, A. J. *Colloid Interface Sci.* **1999**, *217*, 203. (d) Graf, C.; van Blaaderen, A. *Langmuir* **2002**, *18*, 524.
- (6) Neeves, A. E.; Birnboim, M. H. *J. Opt. Soc. Am. B* **1989**, *6*, 787.
- (7) (a) Liz-Marzan, L. M.; Giersig, M.; Mulvaney, P. *Chem. Commun.* **1996**, 731. (b) Giersig, M.; Liz-Marzan, L. M.; Ung, T.; Su, D.; Mulvaney, P. *Ber. Bunsen-Ges. Phys. Chem.* **1997**, *101*, 1617.
- (8) Hardikar, V. V.; Matijevic, E. J. *Colloid Interface Sci.* **2000**, *221*, 133.
- (9) (a) Lu, Y.; Yin, Y.; Mayers, B. T.; Xia, Y. *Nano Lett.* **2002**, *2*, 183. (b) Yin, Y.; Lu, Y.; Sun, Y.; Xia, Y. *Nano Lett.* **2002**, *2*, 427.
- (10) (a) Wang, W.; Asher, S. A. *J. Am. Chem. Soc.* **2001**, *123*, 12528. (b) Velikov, K. P.; Moroz, A.; van Blaaderen, A. *Appl. Phys. Lett.* **2002**, *80*, 49. (c) Rodríguez-González, B.; Salgueiriño-Maceira, V.; García-Santamaría, F.; Liz-Marzán, L. M. *Nano Lett.* **2002**, in press.
- (11) Lu, Y.; Yin, Y.; Gates, B.; Xia, Y. *Langmuir* **2001**, *17*, 6344.
- (12) Liz-Marzan, L. M.; Giersig, M.; Mulvaney, P. *Langmuir* **1996**, *12*, 4329.
- (13) Quinten, M.; Leitner, A.; Krenn, J. R.; Aussenegg, F. R. *Opt. Lett.* **1998**, *23*, 1331.
- (14) Krenn, J. R.; Dereux, A.; Weeber, J. C.; Bourillot, E.; Lacroute, Y.; Goudonnet, J. P.; Schider, G.; Gotschy, W.; Leitner, A.; Aussenegg, F. R.; Giarad, C. *Phys. Rev. Lett.* **1999**, *82*, 2590.
- (15) (a) Brongersma, M. L.; Hartman, J. W.; Atwater, H. A. *Phys. Rev. B* **2000**, *62*, R16356. (b) Wekis, A.; Chen, J. C.; Kurland, I.; Fan, S.; Villeneuve, R.; Joannopoulos, J. D. *Phys. Rev. Lett.* **1996**, *77*, 3787.
- (16) Maier, S. A.; Brongersma, M. L.; Kik, P. G.; Meltzer, S.; Requicha, A. A. G.; Atwater, H. A. *Adv. Mater.* **2001**, *13*, 1501.
- (17) (a) Yin, Y.; Lu, Y.; Gates, B.; Xia, Y. *J. Am. Chem. Soc.* **2001**, *123*, 8718. (b) Yin, Y.; Lu, Y.; Xia, Y. *J. Mater. Chem.* **2001**, *11*, 987. (c) Lee, I.; Zheng, H.; Rubner, M. F.; Hammond, P. T. *Adv. Mater.* **2002**, *14*, 572.
- (18) (a) Aizenberg, J.; Rogers, J. A.; Paul, K. E.; Whitesides, G. M. *Appl. Phys. Lett.* **1997**, *71*, 3773. (b) Yin, Y.; Gates, B.; Xia, Y. *Adv. Mater.* **2000**, *12*, 1426. (c) Li, Z.-Y.; Yin, Y.; Xia, Y. *Appl. Phys. Lett.* **2001**, *78*, 2431.

NL025598I